Thermo-diffusion of a thick circular plate via modified Green–Naghdi models

A. M. ZENKOUR

Department of Mathematics, Faculty of Science, King Abdulaziz University, P.O. Box 80203, Jeddah 21589, Saudi Arabia, e-mail: zenkour@kau.edu.sa
and
Department of Mathematics, Faculty of Science, Kafrelsheikh University, Kafrelsheikh 33516, Egypt, e-mail: zenkour@sci.kfs.edu.eg

THIS ARTICLE PRESENTS THE THERMO-DIFFUSION of an isotropic thick circular plate. The Green and Naghdi's models including the energy dissipation are anticipated in their simple forms. Novel multi single/dual-phase-lag models with higher-order time-derivatives are also provided to examine the thermo-diffusion response of the circular plate. The simple and refined forms of Green and Naghdi's types II and III are investigated in this work. The closed-form solution of thermal diffusion governing equations is attained by taking into account the boundary conditions. A validation examples of outcomes are acceptable by comparing all quantities according to the discussing of all thermoelastic models. The refined forms of Green and Naghdi's types II and III should be applied to get accurate outcomes.

Key words: thermal diffusion, chemical potential, multi-dual-phase-lag, Green and Naghdi II, III.

Notation

a	measure of the thermodiffusion effect,
α_c	linear diffusion expansion coefficient,
α_t	thermal expansion coefficient,
C	concentration,
C_ϑ	specific heat at uniform strain,
D	diffusion coefficient,
$\vec{\nabla}\theta$	temperature gradient,
$\vec{\nabla}\vartheta$	thermal displacement gradient,
$e = u_{k,k}$	cubical dilatation,
e_{ij}	strain tensor components,
ξ	wave number in the radial r-direction,
ϑ	thermal displacement,
$\gamma_1 = (3\lambda + 2\mu)\alpha_t$	thermal modulus,
$\gamma_2 = (3\lambda + 2\mu)\alpha_c$	thermo-diffusion coupling component,
k	heat conductivity coefficient,
k^*	positive constant (rate of thermal conductivity of an isotropic material),
$\lambda,\ \mu$	Lamé's elastic parameters,

∇^2	Laplacian operator,
ω	complex frequency,
P	chemical potential,
$\vec{q}$	heat flux vector,
$r\phi z$	cylindrical polar co-ordinates,
ρ	material density,
σ_{ij}	stress tensor components,
T	thermodynamical temperature,
T_0	environment temperature,
τ_q	phase-lag of heat flux,
τ_θ	phase-lag of temperature gradient,
τ_ϑ	phase-lag of thermal displacement gradient,
$\theta = T - T_0$	temperature change,
$\vec{u} \equiv (u, 0, w)$	displacement vector.

1. Introduction

ALL GENERALIZED THERMOELASTICITY THEORIES are investigated to improve and treat the shortening in the classical one of BIOT [1]. One of the most significant generalized theory is that given by GREEN and NAGHDI (G–N) [2–5]. It includes both $\vec{\nabla}\theta$ and $\vec{\nabla}\vartheta$ among the constitutive quantities. Green and Naghdi presented their heat conduction law in the context of

$$(1.1) \qquad \vec{q}(P,t) = -k\vec{\nabla}\theta(P,t) - k^*\vec{\nabla}\vartheta(P,t).$$

The thermal displacement ϑ is firstly proposed in G–N [5] by the relations

$$(1.2) \qquad \vartheta = \int_{t_0}^{t} \theta(P,s)\,\mathrm{d}s, \quad \frac{\partial\vartheta}{\partial t} = \theta, \quad \vartheta(P,t_0) = 0.$$

The three-phase-lag (TPL) to $\vec{q}$, $\vec{\nabla}\theta$ and $\vec{\nabla}\vartheta$ are introduced to expand G–N law. That is

$$(1.3) \qquad \vec{q}(P,t+\tau_q) = -k\vec{\nabla}\theta(P,t+\tau_\theta) - k^*\vec{\nabla}\vartheta(P,t+\tau_\vartheta),$$

where $0 \le \tau_\vartheta < \tau_\theta < \tau_q$. Then, Eq. (1.3) shows that both $\vec{\nabla}\theta$ and $\vec{\nabla}\vartheta$ known along a material volume found a position $P(\vec{r})$ at time $t + \tau_\theta$ and $t + \tau_\vartheta$ bring about heat flux $\vec{q}$ to stream at additional instantaneous of time τ_q.

Taylor's series expansion may be used of Eq. (1.3) up to high time-derivatives in τ_q, τ_θ and τ_ϑ to yield

$$(1.4) \qquad \left(1 + \sum_{m=1}^{M} \frac{\tau_q^m}{m!} \frac{\partial^m}{\partial t^m}\right)\vec{q} = -k\left(1 + \sum_{n=1}^{N} \frac{\tau_\theta^n}{n!} \frac{\partial^n}{\partial t^n}\right)\vec{\nabla}\theta$$

$$- k^*\left(1 + \sum_{n=1}^{N} \frac{\tau_\vartheta^n}{n!} \frac{\partial^n}{\partial t^n}\right)\vec{\nabla}\vartheta,$$

which fills in as an expansion to the generalized heat conduction formula that neglecting the mechanical term.

To obtain a novel heat conduction equation based on G–N theory we begin with the energy equation for an isotropic thermo-diffusive plate without any heat source and it is stated in the form

$$(1.5) \qquad -\vec{\nabla} \cdot \vec{q} = \frac{\partial}{\partial t}(\rho C_\vartheta \theta + aT_0 C + \gamma_1 T_0 u_{k,k}).$$

If we income the divergence followed by the first derivative with respect to t of both sides of Eq. (1.4) and then using Eq. (1.5) we get

$$(1.6) \qquad \left[k\left(1 + \sum_{n=1}^{N} \frac{\tau_\theta^n}{n!} \frac{\partial^n}{\partial t^n}\right) \frac{\partial}{\partial t} + k^*\left(1 + \sum_{n=1}^{N} \frac{\tau_\vartheta^n}{n!} \frac{\partial^n}{\partial t^n}\right) \right] \nabla^2 \theta$$
$$= \left(1 + \sum_{m=1}^{M} \frac{\tau_q^m}{m!} \frac{\partial^m}{\partial t^m}\right) \frac{\partial^2}{\partial t^2}(\rho C_\vartheta \theta + aT_0 C + \gamma_1 T_0 u_{k,k}),$$

which denotes the modified coupled heat equation that comprises TPL impacts for an isotropic plate. In the following we present some special cases from Eq. (1.6).

The basic formula for the TPL heat conduction equation according to G–N of type III is given by setting $N = 1$ and $M = 2$ in Eq. (1.6). That is

$$(1.7) \qquad \left[k\left(1 + \tau_\theta \frac{\partial}{\partial t}\right) \frac{\partial}{\partial t} + k^*\left(1 + \tau_\vartheta \frac{\partial}{\partial t}\right) \right] \nabla^2 \theta$$
$$= \left(1 + \tau_q \frac{\partial}{\partial t} + \frac{1}{2}\tau_q^2 \frac{\partial^2}{\partial t^2}\right) \frac{\partial^2}{\partial t^2}(\rho C_\vartheta \theta + aT_0 C + \gamma_1 T_0 u_{k,k}),$$

which represents a target heat conduction equation for a lot of investigators [6–21] and many of them may be omitting the term containing τ_q^2.

Also, the "single-phase-lag" (SPL) model according to G–N of type III for an isotropic body is given by putting $M = 1$ and $\tau_\theta = \tau_\vartheta = 0$ in Eq. (1.6). That is

$$(1.8) \qquad \left(k\frac{\partial}{\partial t} + k^*\right) \nabla^2 \theta = \left(1 + \tau_q \frac{\partial}{\partial t}\right) \frac{\partial^2}{\partial t^2}(\rho C_\vartheta \theta + aT_0 C + \gamma_1 T_0 u_{k,k}).$$

Finally, the simple model according to G–N of type III [2–5] is given by setting $\tau_q = \tau_\theta = \tau_\vartheta = 0$ in Eq. (1.6) in the form [22–29]

$$(1.9) \qquad \left(k\frac{\partial}{\partial t} + k^*\right) \nabla^2 \theta = \frac{\partial^2}{\partial t^2}(\rho C_\vartheta \theta + aT_0 C + \gamma_1 T_0 u_{k,k}).$$

Setting $\tau_\theta = 0$ in Eq. (1.7), we get the DPL heat conduction equation according to G–N of type III as

$$(1.10) \qquad \left[k \frac{\partial}{\partial t} + k^* \left(1 + \tau_\vartheta \frac{\partial}{\partial t} \right) \right] \nabla^2 \theta$$
$$= \left(1 + \tau_q \frac{\partial}{\partial t} + \frac{1}{2} \tau_q^2 \frac{\partial^2}{\partial t^2} \right) \frac{\partial^2}{\partial t^2} (\rho C_\vartheta \theta + a T_0 C + \gamma_1 T_0 u_{k,k}).$$

Though, if we set $\tau_q^2 \to 0$ and $k = 0$, then Eq. (1.10) inclines to

$$(1.11) \qquad k^* \left(1 + \tau_\vartheta \frac{\partial}{\partial t} \right) \nabla^2 \theta = \left(1 + \tau_q \frac{\partial}{\partial t} \right) \frac{\partial^2}{\partial t^2} (\rho C_\vartheta \theta + a T_0 C + \gamma_1 T_0 u_{k,k}).$$

The above equation characterizes the DPL G–N type II heat conduction equation [15]. Putting $\tau_\vartheta = \tau_q = 0$, Eq. (1.11) tends to [30–33]

$$(1.12) \qquad k^* \nabla^2 \theta = \frac{\partial^2}{\partial t^2} (\rho C_\vartheta \theta + a T_0 C + \gamma_1 T_0 u_{k,k}).$$

The above formula characterizes a simple heat conduction equation based upon the G–N model of type II which includes k^* instead of k. Equation (1.12) can be expressed from Eq. (1.9) if we set $k = 0$. Also, putting $k^* = 0$ in Eq. (1.9) tends another simple heat equation according to G–N of type II that include k in the form

$$(1.13) \qquad k \nabla^2 \theta = \frac{\partial}{\partial t} (\rho C_\vartheta \theta + a T_0 C + \gamma_1 T_0 u_{k,k}).$$

In what follows we summarize all models by setting a unified DPL Green–Naghdi heat conduction equation ($\tau_\theta \to 0$) in the form (ZENKOUR [35–42]):

$$(1.14) \qquad k \mathcal{L}_\vartheta^1 (\nabla^2 \theta) = \mathcal{L}_q (\rho C_\vartheta \theta + a T_0 C + \gamma_1 T_0 u_{k,k}).$$

where

$$(1.15) \qquad \mathcal{L}_\vartheta^1 = \frac{\partial}{\partial t} + \frac{\epsilon k^*}{k} \left(1 + \sum_{n=1}^{N} \frac{\tau_\vartheta^n}{n!} \frac{\partial^n}{\partial t^n} \right), \qquad \mathcal{L}_q = \left(1 + \sum_{m=1}^{M} \frac{\tau_q^m}{m!} \frac{\partial^m}{\partial t^m} \right) \frac{\partial^2}{\partial t^2}.$$

Here ϵ is a dimensionless key integer, either equals zero or one according to the case chosen. Eq. (1.14) is the most general one when M, N have various positive integer values more than zero. Roughly different models are gained from Eq. (1.14) in the following form:

- DPL G–N of type III: $\epsilon = 1$, $M = N \geq 1$.
- SPL G–N of type III: $\epsilon = 1$, $M = 1$, $\tau_\vartheta = 0$.

- SPL G–N of type II: $\epsilon = 0$, $M = 1$, $\tau_\vartheta = 0$.
- Simple G–N of type III: $\epsilon = 1$, $\tau_q = \tau_\vartheta = 0$.
- Simple G–N of type II: $\epsilon = 0$, $\tau_q = \tau_\vartheta = 0$.

The present article is concerned with the study of diffusion phenomenon. OTHMAN *et al.* [43] discussed the impact of diffusion on 2D problem of generalized thermoelasticity with G–N model. SINGH [44] proposed the wave propagation in a thermoelastic solid with diffusion via G–N theory. DESWAL and KALKAL [45] presented the electromagneto-thermodiffusive problem for short times using G–N theory without energy dissipation. HOSSEINI *et al.* [46] presented a 2D transient analysis of coupled non-Fick diffusion-thermoelasticity based on G–N theory using the meshless local Petrov–Galerkin method. TRIPATHI *et al.* [47] discussed the generalized thermoelastic diffusion in thick plates with axisymmetric heat supply. SINGH *et al.* [48] presented the reflection of plane waves in thermo-diffusion elasticity via G–N theory without dissipation taken into account the rotation effect. XIONG and TIAN [49] dealt with the response of transient magneto-thermo-elasto-diffusive of rotating porous media without energy dissipation under thermal shock. AOUADI *et al.* [50] studied the bending theory of thermoelastic diffusion plates based on G–N theory. AOUADI *et al.* [51] proposed a porous thermoelastic diffusion theory according to G–N theory of types II and III. LAZZARI and NIBBI [52] discussed the energy decay in G–N thermoelasticity with diffusion and dissipative boundary controls.

A lot of cases based upon Green and Naghdi's and the phase-lag theories are adopted to deal with the basic equations of the thermoelastic diffusion circular plates. The exact solutions for different fields "like temperature, dilatation, displacements, concentration, stresses, and chemical potential" are investigated. The boundary conditions at the upper and lower surfaces of the circular plate are taken into account. The validation and applications of the problem are discussed by comparing the modified models with the simple ones. At long last, a general conversation about the picked up outcomes is accounted for together with ends and future perspectives. Some classified outcomes are introduced to help different agents in their applications.

2. Basic equations

Let us consider a thermo-diffusion behavior on a 2D half-space circular plate using a combination of the multi-phase-lag and Green and Naghdi's theories. The normal z-axis is taken as the axis of symmetry and the origin of the system of co-ordinates is at the mid-plane between surfaces of the plate. The problem is outlined according to the cylindrical polar co-ordinates (r, φ, z). All functions rely upon the time t and the radial and normal coordinates x and z. The last

type of the heat conduction formula is introduced in Eq. (1.14). The plate is of infinite extent in the radial direction and has finite thickness. The thickness of the plate is $2h$ and it is occupying the region

(2.1) $$R = \{(r, \varphi, z) : 0 \leq r \leq \infty, \; -h \leq z \leq h\}.$$

The displacement vector $\vec{u} \equiv (u, 0, w)$ for the 2D problem is considered. The strain tensor components are given by

(2.2) $$e_{rr} = \frac{\partial u}{\partial r}, \quad e_{\varphi\varphi} = \frac{u}{r}, \quad e_{zz} = \frac{\partial w}{\partial z}, \quad e_{rz} = \frac{1}{2}\left(\frac{\partial w}{\partial r} + \frac{\partial u}{\partial z}\right),$$

and $e = u_{k,k}$ is represented by

(2.3) $$e = \frac{\partial u}{\partial r} + \frac{u}{r} + \frac{\partial w}{\partial z} = \frac{1}{r}\frac{\partial}{\partial r}(ru).$$

The dynamic equations without body forces are represented by

(2.4)
$$\mu\left(\nabla^2 u - \frac{u}{r^2}\right) + (\lambda + \mu)\frac{\partial e}{\partial r} - \gamma_1\frac{\partial \theta}{\partial r} - \gamma_2\frac{\partial C}{\partial r} = \rho\frac{\partial^2 u}{\partial t^2},$$
$$\mu\nabla^2 w + (\lambda + \mu)\frac{\partial e}{\partial z} - \gamma_1\frac{\partial \theta}{\partial z} - \gamma_2\frac{\partial C}{\partial z} = \rho\frac{\partial^2 w}{\partial t^2},$$

where

(2.5) $$\nabla^2 = \frac{\partial^2}{\partial r^2} + \frac{1}{r}\frac{\partial}{\partial r} + \frac{\partial^2}{\partial z^2}.$$

The equation of mass diffusion can be expressed by

(2.6) $$L_\vartheta^0(C) = D\nabla^2 P, \quad L_\vartheta^0 = \left(1 + \sum_{n=1}^{N-1}\frac{\tau_\vartheta^n}{n!}\frac{\partial^n}{\partial t^n}\right)\frac{\partial}{\partial t}.$$

According to the Duhamel-Neumann formulae, the stress-strain-temperature-diffusion relations for the present medium with dismissing the body forces can be communicated in the form

(2.7)
$$\sigma_{rr} = 2\mu\frac{\partial u}{\partial r} + \lambda e - \gamma_1\theta - \gamma_2 C,$$
$$\sigma_{\varphi\varphi} = 2\mu\frac{u}{r} + \lambda e - \gamma_1\theta - \gamma_2 C,$$
$$\sigma_{zz} = 2\mu\frac{\partial w}{\partial z} + \lambda e - \gamma_1\theta - \gamma_2 C,$$
$$\sigma_{zr} = \mu\left(\frac{\partial w}{\partial r} + \frac{\partial u}{\partial z}\right), \quad \sigma_{r\varphi} = \sigma_{\varphi z} = 0,$$

(2.8) $$P = bC - \gamma_2 e - a\theta.$$

Using Eq. (2.8) into Eq. (2.6), we get the diffusion equation as

(2.9) $$\mathcal{L}_\vartheta^0(C) - D\nabla^2(bC - \beta e - a\theta) = 0.$$

3. Formulation of the problem

It is reasonable to introduce the accompanying dimensionless variables in the following parts:

(3.1)
$$\{r', z', u', w'\} = c_0\eta\{r, z, u, w\}, \quad \{t', \tau'_\vartheta, \tau'_q\} = \eta c_0^2\{t, \tau_\vartheta, \tau_q\},$$

$$(k^*)' = \frac{k^*}{k\eta c_0^2}, \quad \theta' = \frac{\beta_1\theta}{\rho c_0^2}, \quad \sigma'_{ij} = \frac{\sigma_{ij}}{\rho c_0^2},$$

$$C' = \frac{\beta_2 C}{\rho c_0^2}, \quad P' = \frac{P}{\beta_2}, \quad c_0^2 = \frac{\lambda + 2\mu}{\rho}, \quad \eta = \frac{\rho C_\vartheta}{k}.$$

According to the above dimensionless factors, one can get the following system of equations (dropping the dashed for comfort):

(3.2)
$$\sigma_{rr} = \frac{\partial u}{\partial r} + c_1\left(\frac{u}{r} + \frac{\partial w}{\partial z}\right) - \theta - C,$$

(3.3)
$$\sigma_{\varphi\varphi} = \frac{u}{r} + c_1\left(\frac{\partial u}{\partial r} + \frac{\partial w}{\partial z}\right) - \theta - C,$$

(3.4)
$$\sigma_{zz} = \frac{\partial w}{\partial z} + c_1\left(\frac{\partial u}{\partial r} + \frac{\partial w}{\partial z}\right) - \theta - C,$$

(3.5)
$$\sigma_{zr} = c_2\left(\frac{\partial w}{\partial r} + \frac{\partial u}{\partial z}\right),$$

(3.6)
$$P = c_3 C - e - c_4\theta,$$

(3.7)
$$\nabla^2 u - \frac{u}{r^2} + c_5\frac{\partial e}{\partial r} - c_6\left(\frac{\partial\theta}{\partial r} + \frac{\partial C}{\partial r} + \frac{\partial^2 u}{\partial t^2}\right) = 0,$$

(3.8)
$$\nabla^2 w + c_5\frac{\partial e}{\partial z} - c_6\left(\frac{\partial\theta}{\partial z} + \frac{\partial C}{\partial z} + \frac{\partial^2 w}{\partial t^2}\right) = 0,$$

(3.9)
$$\mathcal{L}^1_\vartheta(\nabla^2\theta) = \mathcal{L}_q(\theta + c_7 C + c_8 e),$$

(3.10)
$$c_9\mathcal{L}^0_\vartheta(C) - \nabla^2(c_3 C - e - c_4\theta) = 0,$$

where

(3.11)
$$c_1 = \frac{\lambda}{\lambda + 2\mu}, \quad c_2 = \frac{\mu}{\lambda + 2\mu}, \quad c_3 = \frac{b(\lambda + 2\mu)}{\gamma_2^2}, \quad c_4 = \frac{a(\lambda + 2\mu)}{\gamma_1\gamma_2},$$

$$c_5 = \frac{1}{c_2}, \quad c_6 = c_5 + 1, \quad c_7 = \frac{aT_0\gamma_1}{\rho C_\vartheta\gamma_2}, \quad c_8 = \frac{\gamma_1^2 T_0}{\rho(\lambda + 2\mu)C_\vartheta},$$

$$c_9 = \frac{(\lambda + 2\mu)k}{D\gamma_2^2\rho C_\vartheta}, \quad \mathcal{L}^1_\vartheta = \frac{\partial}{\partial t} + \epsilon k^*\left(1 + \sum_{n=1}^{N}\frac{\tau_\vartheta^n}{n!}\frac{\partial^n}{\partial t^n}\right).$$

4. Closed-form solution

To obtain the total arrangements of all fields, we initially apply the accompanying boundary conditions:

$$\left.\frac{\partial \theta}{\partial z}\right|_{z=\pm h} = \pm \theta_0 f(r,t), \quad \sigma_{zz} = \sigma_{rz} = 0 \quad \text{at } z = \pm h,$$

(4.1)

$$P = P_0 f(r,t) \quad \text{at } z = -h.$$

On simplifying Eqs. (3.7) and (3.8), we obtain

(4.2)
$$\left(\nabla^2 - \frac{\partial^2}{\partial t^2}\right)e - \nabla^2(\theta + C) = 0.$$

The solution of all quantities can be derived by applying the normal modes

(4.3)
$$\{\theta, C, e\}(r,z,t) = \{\theta^*, C^*, e^*\}(z)e^{(i\xi r + \omega t)},$$

where $i = \sqrt{-1}$ and $\theta^*(z)$, $C^*(z)$, and $e^*(z)$ denote the amplitudes of the corresponding field variables. Using Eq. (4.3), then the governing equations, Eqs. (4.2), (3.9), (3.10), became

(4.4)
$$(\mathcal{D}^2 - a_1)(\theta^* + C^*) + (\mathcal{D}^2 - a_2)e^* = 0,$$

(4.5)
$$(\mathcal{D}^2 - a_3)\theta^* - a_4 C^* - a_5 e^* = 0,$$

(4.6)
$$c_4(\mathcal{D}^2 - a_1)\theta^* - (c_3\mathcal{D}^2 - c_7)C^* + (\mathcal{D}^2 - a_1)e^* = 0,$$

where

(4.7)
$$\mathcal{D} = \frac{d}{dz}, \quad a_1 = \frac{\xi(\xi r - i)}{r}, \quad a_2 = a_1 + \omega^2, \quad a_3 = a_1 + \frac{\bar{\mathcal{L}}_q}{\bar{\mathcal{L}}_\vartheta^1},$$

$$\{a_4, a_5\} = \frac{\bar{\mathcal{L}}_q}{\bar{\mathcal{L}}_\vartheta^1}\{c_7, c_8\}, \quad a_6 = a_1 c_3 + c_9 \bar{\mathcal{L}}_\vartheta^0,$$

in which

(4.8)
$$\bar{\mathcal{L}}_q = \omega^2\left(1 + \sum_{m=1}^{M} \frac{\tau_q^m}{m!}\omega^m\right), \quad \bar{\mathcal{L}}_\vartheta^0 = \omega\left(1 + \sum_{n=1}^{N-1} \frac{\tau_\vartheta^n}{n!}\omega^n\right),$$

$$\bar{\mathcal{L}}_\vartheta^1 = \omega + \epsilon k^*\left(1 + \sum_{n=1}^{N} \frac{\tau_\vartheta^n}{n!}\omega^n\right).$$

Equations (4.4)–(4.6) can be rearranged in six-order ordinary, homogenous, differential equations in $\theta^*(z)$, $C^*(z)$ and $e^*(z)$ which can be written as:

(4.9)
$$(D^6 - A_2 D^4 + A_1 D^2 - A_0)\{\theta^*, C^*, e^*\}(z) = 0,$$

where the coefficients A_i are given by

$$A_0 = \frac{a_1^2(a_3 - a_4 - a_5 c_4) + a_1 a_2 a_4 c_4 - a_1 a_5 a_6 + a_2 a_3 a_6}{1 + c_3},$$

(4.10) $\quad A_1 = \frac{a_1 a_4 c_4 - a_1 a_5 (c_3 + 2c_4) + a_2(a_3 c_3 + a_4 c_4) + a_1^2 + 2a_1(a_3 - a_4) + (a_2 + a_3 - a_5)a_6}{1 + c_3},$

$$A_2 = \frac{(a_2 + a_3 - a_5)c_3 + (a_4 - a_5)c_5 + 2a_1 + a_4 - a_4 + a_6}{1 + c_3}.$$

The general solutions of Eqs. (4.10) can be stated in the form

(4.11) $$\{\theta^*, C^*, e^*\}(z) = \sum_{j=1}^{3} \{B_n, B_n', B_n''\} e^{-s_j z},$$

where B_j, B_j' and B_j'' are the integration constants and s_j $(j = 1, 2, 3)$ are positive roots of the typical equation

(4.12) $$s_j^6 - A_2 s_j^4 + A_1 s_j^2 - A_0 = 0.$$

They are given, respectively, by

(4.13)
$$s_1 = \sqrt{\frac{1}{3}[A_2 + 2p_1 \sin(p_2)]},$$

$$s_{2,3} = \sqrt{\frac{1}{3}\{A_2 \mp p_1[\sqrt{3}\cos(p_2) \pm \sin(p_2)]\}},$$

in which

(4.14) $\quad p_1^2 = A_2^2 - 3A_1, \quad p_2 = \frac{1}{3}\sin^{-1}(p_0), \quad p_0 = \frac{9A_1 A_2 - 2A_2^3 - 27A_0}{2p_1^3}.$

The relations between the parameters B_n, B_n' and B_n'' can be obtained by using Eq. (4.11) into Eqs. (4.4) and (4.5):

(4.15) $$\{B_j', B_j''\} = \{\beta_{1j}, \beta_{2j}\}B_j, \quad j = 1, 2, 3,$$

where

(4.16) $$\beta_{1j} = \frac{a_1 s_j(a_5 - a_4)}{a_1 a_6 - a_3 a_5}, \beta_{2j} = -\frac{s_j(a_1 a_6 - a_3 a_4)}{a_1 a_6 - a_3 a_5}.$$

Presently, the temperature, concentration and dilatation can be expressed in the last form as

(4.17) $$\{\theta, C, e\}(r, z, t) = \sum_{j=1}^{3} B_j\{1, \beta_{1j}, \beta_{2j}\} e^{-s_j z}.$$

The radial and axial displacement components can be obtained by using Eq. (4.11) in Eqs. (3.7) and (3.8) in the form

(4.18)
$$u(r, z, t) = B_4 \cos(u_0 z) + B_5 \sin(u_0 z) + i\xi \sum_{j=1}^{3} \beta_{3j} B_j e^{-s_j z},$$

$$w(r, z, t) = B_6 \cos(w_0 z) + B_7 \sin(w_0 z) - \sum_{j=1}^{3} s_j \beta_{3j} B_j e^{-s_j z},$$

where

(4.19)
$$u_0^2 = \frac{i\xi}{r} - \frac{1}{r^2} - \xi^2 - c_6 \omega^2, \quad w_0^2 = u_0^2 + \frac{1}{r^2},$$

$$\beta_{3j} = \frac{(a_4 - a_5)(a_1 a_5 + a_3 a_6)}{(a_1 a_6 - a_3 a_5)(u_1^2 + s_j^2)}.$$

Then, it is easily given the stresses and chemical potential in terms of the displacements, temperature, dilatation and concentration.

The boundary conditions appeared in Eq. (4.1) may be applied with $f(r, t) = e^{(i\xi r + \omega t)}$ to get the seven parameters B_j and therefore the final form of all the variable quantities.

5. Numerical results

Some application and validation examples are presented to put into suggestion the impact of different models on the field variables. Material properties of a metal material are introduced here

$\lambda = 7.76 \times 10^{10} \text{ N} \cdot \text{m}^{-2}, \quad \mu = 3.86 \times 10^{10} \text{ N} \cdot \text{m}^{-2},$

$k = 386 \text{ W} \cdot \text{m}^{-1} \cdot \text{K}^{-1}, \quad \rho = 8954 \text{ kg} \cdot \text{m}^{-3}, \quad \alpha_t = 1.78 \times 10^{-5} \text{ K}^{-1},$

$\alpha_c = 1.98 \times 10^{-4} \text{ m}^3 \cdot \text{kg}^{-1}, \quad C_\vartheta = 383.1 \text{ J} \cdot \text{kg}^{-1} \cdot \text{K}^{-1}, \quad T_0 = 293 \text{ K},$

$D = 0.85 \times 10^{-8} \text{ kg} \cdot \text{s} \cdot \text{m}^{-3}, \quad k^* = 1.2, \quad a = 1.2 \times 10^4 \text{ m}^2 \cdot \text{s}^{-2} \cdot \text{K}^{-1},$

$b = 0.9 \times 10^6 \text{ m}^2 \cdot \text{s}^{-2} \cdot \text{K}^{-1}.$

For comfort, the absolute values of the accompanying thermoelastic amounts have been received to speak of the outcomes:

$$\{\bar{\theta}, \bar{w}, \bar{C}, \sigma_4\} = \frac{1}{\theta_0} \{\theta, w, C, \sigma_{13}\}(r, z, t), \quad \bar{P} = \frac{1}{\theta_0^3} P(r, z, t),$$

$$\{\bar{u}, \sigma_1, \sigma_2, \sigma_3\} = \frac{1}{\theta_0^2} \{u, \sigma_{11}, \sigma_{22}, \sigma_{33}\}(r, z, t).$$

Numerical results are obtained for $P_0 = 150$, $\theta_0 = 10$, $\omega_0 = 1.95$, $\omega_1 = 0.05$, $\xi = \pi/3$, $\tau_q = 0.1$, $\tau_\vartheta = 0.05$, $r = 4$, $h = 0.8$ and $t = 0.3$.

Results of the temperature, dilatation, displacements and concentration due to simple G–N of type II, SPL G–N of type II, simple G–N of type III, SPL G–N of type III and DPL G–N of type III thermoelasticity models are presented in Tables 1 and 2 for $\bar{z} = 0.5$. Similar results of the stresses and chemical potential are reported in Tables 3 and 4. Additional sample graphs are plotted in Figs. 1–10 through the circular plate thickness to show the impact of all models on the field variables. In Tables 1–4, the relative error is presented between two parentheses and calculated according to the formula

$$\left(\frac{\text{simple value} - \text{modified value}}{\text{modified value}} \right) \times 100\%.$$

Table 1. Effect of G–N II thermoelasticity theories on temperature, dilatation, displacements and concentration of the thicker circular plate.

		$\bar{\theta}$	$\bar{e}$	$\bar{u}$	$\bar{w}$	$\bar{C}$
	Simple	4.872802	1.679656	3.876542	2.636469	4.831283
SPL	$N = 1$	4.580739	1.888093	3.026801	2.003210	4.528736
	$N = 2$	4.556325	1.908020	2.961713	1.973270	4.503267
	$N = 3$	4.554772	1.909317	2.957580	1.971346	4.501646
	$N = 4$	4.554697	1.909380	2.957380	1.971247	4.501568
	$N = 5$	4.554694	1.909382	2.957372	1.971243	4.501565
		(6.98%)	(−12.03%)	(31.08%)	(33.74%)	(7.32%)
	$N = 6$	4.554694	1.909383	2.957372	1.971243	4.501565

Table 2. Effect of G–N III thermoelasticity theories on temperature, dilatation, displacements and concentration of the thicker circular plate.

		$\bar{\theta}$	$\bar{e}$	$\bar{u}$	$\bar{w}$	$\bar{C}$
	Simple	5.796679	1.235940	7.630031	8.521795	5.773355
SPL	$N = 1$	5.439970	1.386453	5.934660	5.411628	5.411411
	$N = 2$	5.409577	1.400672	5.804331	5.189524	5.380498
	$N = 3$	5.407646	1.401597	5.796060	5.175372	5.378534
	$N = 4$	5.407553	1.401642	5.795659	5.174678	5.378439
	$N = 5$	5.407550	1.401644	5.795643	5.174650	5.378436
		(7.20%)	(-11.82%)	(31.65%)	(64.68%)	(7.34%)
	$N = 6$	5.407550	1.401644	5.795643	5.174649	5.378436
DPL	$N = 1$	5.511926	1.354389	6.248526	5.950472	5.484550
	$N = 2$	5.476047	1.361448	6.117328	5.694611	5.448331
	$N = 3$	5.473797	1.362043	6.108669	5.678119	5.446057
	$N = 4$	5.473693	1.362078	6.108244	5.677322	5.445952
	$N = 5$	5.473689	1.362079	6.108228	5.677291	5.445948
		(5.90%)	(−9.26%)	(24.91%)	(50.10%)	(6.01%)
	$N = 6$	5.473689	1.362080	6.108227	5.677290	5.445947

Table 3. Effect of G–N II thermoelasticity theories on stresses and chemical potential of the thicker circular plate.

		σ_1	σ_2	σ_3	σ_4	$\bar{P}$
	Simple	5.277423	3.355263	4.441777	1.144026	2.053667
SPL	$N = 1$	4.114443	2.613374	3.454152	0.833648	1.925748
	$N = 2$	4.025357	2.556547	3.378473	0.816412	1.914988
	$N = 3$	4.019700	2.552939	3.373667	0.815308	1.914304
	$N = 4$	4.019426	2.552764	3.373434	0.815252	1.914271
	$N = 5$	4.019415	2.552757	3.373425	0.815250	1.914270
		(31.30%)	(31.30%)	(31.67%)	(40.32%)	(7.28%)
	$N = 6$	4.019415	2.552757	3.373425	0.815249	1.914269

Table 4. Effect of G–N III thermoelasticity theories on stresses and chemical potential of the thicker circular plate.

		σ_1	σ_2	σ_3	σ_4	$\bar{P}$
	Simple	10.411435	6.630057	8.795727	3.548307	2.452755
SPL	$N = 1$	8.092957	5.151280	6.830322	2.305653	2.299332
	$N = 2$	7.914679	5.037564	6.679129	2.216085	2.286232
	$N = 3$	7.903364	5.030347	6.669533	2.210377	2.285400
	$N = 4$	7.902816	5.029997	6.669067	2.210097	2.285360
	$N = 5$	7.902794	5.029984	6.669049	2.210086	2.285358
		(31.74%)	(31.81%)	(31.89%)	(60.55%)	(7.32%)
	$N = 6$	7.902794	5.029983	6.669049	2.210086	2.285358
DPL	$N = 1$	8.522240	5.425096	7.194321	2.522531	2.330328
	$N = 2$	8.342830	5.310655	7.042247	2.420561	2.314966
	$N = 3$	8.330986	5.303100	7.032205	2.413974	2.314001
	$N = 4$	8.330405	5.302730	7.031713	2.413655	2.313957
	$N = 5$	8.330383	5.302716	7.031694	2.413643	2.313955
		(24.98%)	(25.03%)	(25.09%)	(47.01%)	(6.00%)
	$N = 6$	8.330382	5.302715	7.031693	2.413643	2.313955

According to Tables 1-4, it can be concluded that:

- The SPL G–N of type II should be applied with $N = 5$ to get more accurate results. So, we present the relative errors at this value only. The relative errors increase as N decreases.
- Also, the SPL G–N of type III or DPL G–N of type III should be applied with $N = 5$ to obtain more precise outcomes
- The SPL G–N of type II, SPL G–N of type III and DPL G–N of type III models produce large field variables except dilatation comparing with the simple G–N of types II and III models.

- For SPL or DPL models the results decrease (increases for dilatation only) as N increases. The decreasing (increasing for dilatation only) amounts may be vanished for $N \geq 5$
- The SPL G–N of type II SPL G–N of type III and DPL G–N of type III give temperature, concentration and chemical potential with the smallest relative error comparing with the simple models
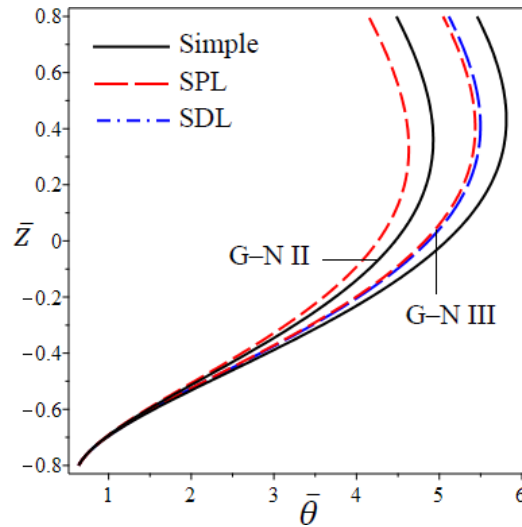
FIG. 1. Effect of G–N models on the temperature $\bar{\theta}$ through the circular plate thickness.
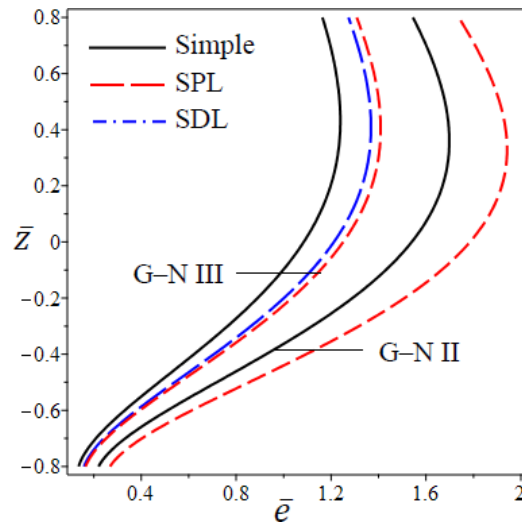
FIG. 2. Effect of G–N models on the dilatation $\bar{e}$ through the circular plate thickness.

- The dilatation possesses negative moderate relative errors.

- The radial, hoop and axial stresses possess large relative errors (about 24%–32%) while the shear stress possesses the highest relative errors (about 40%–61%).
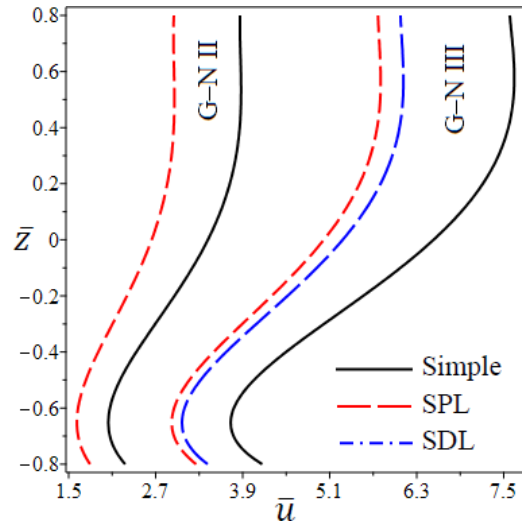
FIG. 3. Effect of G–N models on the radial displacement $\bar{u}$ through the circular plate thickness.
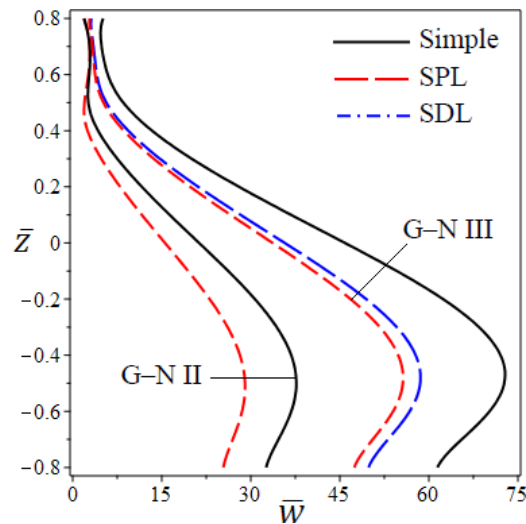
FIG. 4. Effect of G–N models on the axial displacement $\bar{w}$ through the circular plate thickness.

Now, Figs. 1–10 are presented as a sample to illustrate the effect of all models on the field quantities along the thickness $\bar{z} = z/h$ of the circular plate. In Fig. 1, the temperature increases through the plate thickness up to the plane $\bar{z} \cong 0.4$ in which $\bar{\theta}$ has its maximum values. The relative error between models increases as $\bar{z}$ increases. Also, the simple and refined G–N of type III models gives the largest temperature $\bar{\theta}$.
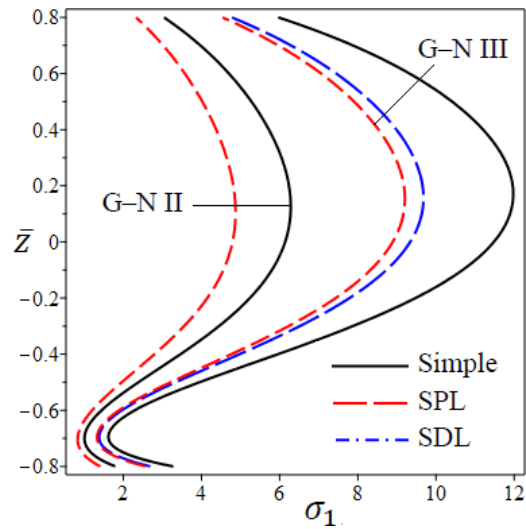
FIG. 5. Effect of G–N models on the radial stress σ_1 through the circular plate thickness.
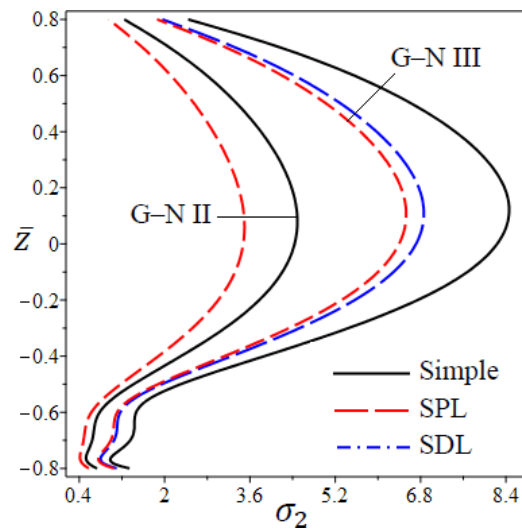
FIG. 6. Effect of G–N models on the hoop stress σ_2 through the circular plate thickness.

Figure 2 shows that the dilatation $\bar{e}$ increases through the plate thickness up to the plane $\bar{z} \cong 0.3$ in which $\bar{e}$ has its maximum values. The relative error between models increases as $\bar{z}$ increases. Also, the simple and refined G–N of type III models gives the smallest dilatation $\bar{e}$.

Figure 3 shows that the radial displacement $\bar{u}$ increases through the plate thickness up to the plane $\bar{z} \cong 0.5$ and above in which $\bar{u}$ has its maximum values
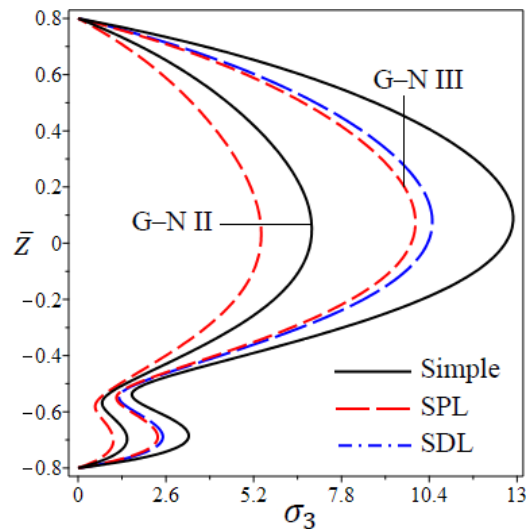
FIG. 7. Effect of G–N models on the axial stress σ_3 through the circular plate thickness.
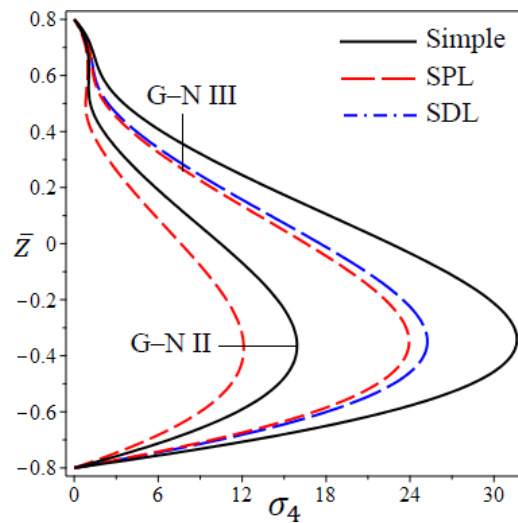
FIG. 8. Effect of G–N models on the shear stress σ_4 through the circular plate thickness.

while $\bar{u}$ has its minimum values at $\bar{z} \cong -0.65$. Once again, the relative error between models increases as $\bar{z}$ increases. Also, the simple and refined G–N of type III models gives the greatest radial displacement $\bar{u}$.

Figure 4 shows that the axial displacement $\bar{w}$ increases through the plate thickness down to the plane $\bar{z} \cong -0.475$ in which $\bar{w}$ has its maximum values
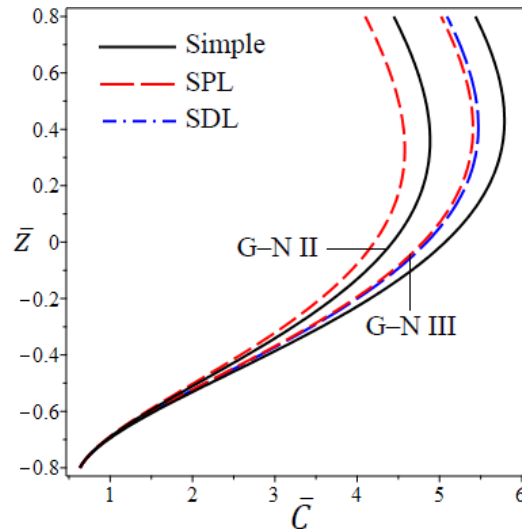
FIG. 9. Effect of G–N models on the concentration $\bar{C}$ through the circular plate thickness.
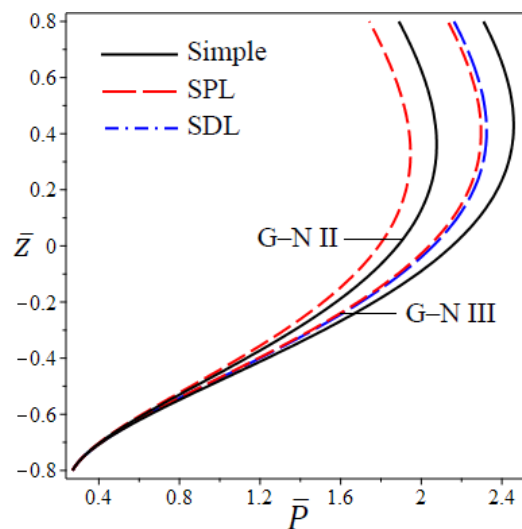
FIG. 10. Effect of G–N models on the chemical potential $\bar{P}$ through the circular plate thickness.

while $\bar{w}$ has its minimum near to the upper face. The relative error between models increases as $\bar{z}$ decreases. Also, the simple and refined G–N of type III models gives the greatest axial displacement $\bar{w}$.

Figures 5 and 6 show that the radial σ_1 and hoop σ_2 stresses have similar behaviors through the plate thickness. The maximum values of radial stress σ_1 occur at $\bar{z} \cong 0.173$ and those of σ_2 occur at $\bar{z} \cong 0.12$. However, the smallest stresses occur near the lower surface; at $\bar{z} = 0.15$ for σ_1 and at $\bar{z} = 0.12$ for σ_2. The simple and refined G–N of type III models gives the greatest stresses σ_1 and σ_2.

Figures 7 and 8 show the axial σ_3 and shear σ_4 stresses through the thickness of the circular plate. Both the axial σ_3 and shear σ_4 stresses vanish at the lower and upper surfaces of the plate to satisfy the boundary conditions at the lower and upper surfaces of the plate. However, the maximum values of σ_3 occur at $\bar{z} \cong 0.075$ and the maximum values of σ_4 occur at $\bar{z} \cong -0.35$. The simple and refined G–N of type III models gives the greatest axial σ_3 and shear σ_4 stresses.

Figures 9 and 10 show that the concentration $\bar{C}$ and the chemical potential $\bar{P}$ have similar behaviors through the plate thickness. The maximum values of concentration $\bar{C}$ occur at $\bar{z} \cong 0.4$ and those of chemical potential $\bar{P}$ occur at $\bar{z} \cong 0.42$. However, the smallest values of both $\bar{C}$ and $\bar{P}$ occur at the lower surface of the circular plate. The simple and refined G–N of type III models gives the greatest concentration and chemical potential.

So, it is concluded for all variable field quantities, except for dilatation, that the SPL G–N of type II gives the smallest quantity while the simple G–N of type III gives the greatest one. However, the SPL G–N of type II gives the greatest dilatation while the simple G–N of type III gives the smallest one. The DPL G–N of type III yields results intermediate those of SPL G–N of type III and the simple G–N of type III. The behaviors are the same for the temperature $\bar{\theta}$, the dilatation $\bar{e}$, the concentration $\bar{C}$, and the chemical potential $\bar{P}$. All these quantities start with zero values then they are no longer increasing through the circular plate thickness and get their maximum values at different positions.

6. Conclusions

The models of Green and Naghdi of types II and III are extended here to obtain novel and exact models of single- and dual-phase-lag of higher-order time-derivative multi terms. The heat of mass diffusion formula just as the constitutive conditions for stresses and chemical potential are provided to the plan of the present issue. The framework is understood, and all field variables are got for the thermal diffusion of a limited thick circular plate. Some approval illustrations are introduced to analyze the straightforward and adjusted Green–Naghdi models. The illustration plots are presented for all variable quantities through the circular

plate thickness. The single-phase-lag Green–Naghdi of type II model gives the smallest field quantity, except dilatation, while the simple Green–Naghdi of type III model gives the greatest one. It is to be noted that the dual-phase lag G–N of type III model yields results intermediate between those of the single-phase-lag Green–Naghdi of type III and the simple Green–Naghdi of type III models. Some outcomes are reported in tables to serve as benchmarks for future comparisons with other researchers.

References

1. M. Biot, *Thermoelasticity and irreversible thermodynamics*, Journal of Applied Physics, **27**, 240–253, 1956.

2. A.E. Green K.A. Lindsay, *Thermoelasicity*, Journal of Elasticity, **2**, 1–7, 1972.

3. A.E. Green, P.M. Naghdi, *A re-examination of the basic postulates of thermomechanics*, Proceedings of The Royal Society of London A, **432**, 171–194, 1991.

4. A.E. Green, P.M. Naghdi, *On undamped heat waves in an elastic solid*, Journal of Thermal Stresses, **15**, 253–264, 1992.

5. A.E. Green, P.M. Naghdi, *Thermoelasticity without energy dissipation*, Journal of Elasticity, **31**, 189–208, 1993.

6. S.K. Roy Choudhuri, *On a thermoelastic three-phase-lag model*, Journal of Thermal Stresses, **30**, 231–238, 2007.

7. R. Quintanilla, R. Racke, *A note on stability in three-phase-lag heat conduction*, International Journal of Heat and Mass Transfer, **51**, 24–29, 2008.

8. A. Kar, M. Kanoria, *Generalized thermoelastic functionally graded orthotropic hollow sphere under thermal shock with three-phase-lag effect*, European Journal of Mechanics – A/Solids, **1**, 1–11, 2009.

9. S. Mukhopadhyay, R. Kumar, *Effect of three phase lag on generalized thermoelasticity for an infinite medium with a cylindrical cavity*, Journal of Thermal Stresses, **32**, 1149–1165, 2009.

10. S. Mukhopadhyay, S. Kothari, R. Kumar, *On the representation of solutions for the theory of generalized thermoelasticity with three phase-lags*, Acta Mechanica, **214**, 305–314, 2010.

11. R. Kumar, V. Chawla, *A study of plane wave propagation in anisotropic three-phase-lag and two-phase-lag model*, International Communications. Heat Mass Transfer, **38**, 1262–1268, 2011.

12. A. Miranville, R. Quintanilla, *A phase-field model based on a three-phase-lag heat conduction*, Applied Mathematics and Optimization, **63**, 133–150, 2011.

13. S. Banik, M. Kanoria, *Effects of three-phase-lag on two-temperature generalized thermoelasticity for infinite medium with spherical cavity*, Applied Mathematics and Mechanics, English Edition, **33**, 4, 483–498, 2012.

14. P. Das, M. Kanoria, *Magneto-thermo-elastic response in a perfectly conducting medium with three-phase-lag effect*, Acta Mechanica, **223**, 4, 811–828, 2012.

15. A.S. El-Karamany, M.A. Ezzat, *On the three-phase-lag linear micropolar thermoelasticity theory*, European Journal of Mechanics – A/Solids, **40**, 198–208, 2013.

16. M.I.A. Othman, S.M. Said, *2D problem of magneto-thermoelasticity fiber-reinforced medium under temperature dependent properties with three-phase-lag model*, Meccanica, **49**, 5, 1225–1241, 2014.

17. R. Kumar, M. Kaur S.C. Rajvanshi, *Reflection and transmission between two micropolar thermoelastic half-spaces with three-phase-lag model* Journal of Engineering Physics and Thermophysics, **87**, 2, 295–307, 2014.

18. S.M. Said, *Influence of gravity on generalized magneto-thermoelastic medium for three-phase-lag model*, Journal of Computational and Applied Mathematics, **291**, 142–157, 2016.

19. S. Biswas, B. Mukhopadhyay, S. Shaw, *Thermal shock response in magneto-thermoelastic orthotropic medium with three-phase-lag model*, Journal of Electromagnetic Waves and Applications, **31**, 9, 879–897, 2017.

20. A.M. Zenkour, M.A. Kutbi, *Multi thermal relaxations for thermodiffusion responses in a thermoelastic half-space*, International Journal of Heat and Mass Transfer, **143**, 118568, 2019.

21. A.M. Zenkour, D.S. Mashat, *A laser pulse impactful on a half-space using the modified TPL G–N models*, Scientific Reports, **10**, 4417, 1–12, 2020.

22. M.I.A. Othman, I.A. Abbas, *Thermal shock problem in a homogeneous isotropic hollow cylinder with energy dissipation*, Computational Mathematics and Modeling, **22**, 3, 266–277, 2011.

23. M.I.A. Othmann, S.Y. Atwa, *Response of micropolar thermoelastic solid with voids due to various sources under Green Naghdi theory,* Acta Mechanica Solida Sinica, **25**, 2, 197–209, 2012.

24. M.I.A. Othman, S.Y. Atwa, *Two-dimensional problem of a fibre-reinforced anisotropic thermoelastic medium. Comparison with the Green–Naghdi theory*, Computational Mathematics and Modeling, **24**, 2, 307–325, 2013.

25. I.A. Abbas, *A GN model for thermoelastic interaction in an unbounded fiber-reinforced anisotropic medium with a circular hole*, Applied Mathematics Letters, **26**, 232–239, 2013.

26. I.A. Abbas, *A GN model based upon two-temperature generalized thermoelastic theory in an unbounded medium with a spherical cavity*, Applied Mathematics and Computation, **245**, 108–115, 2014.

27. A.S. El-Karamany, M.A. Ezzat, *Two-temperature Green–Naghdi theory type III in linear thermoviscoelastic anisotropic solid*, Applied Mathematical Modelling, **39**, 2155–2171, 2015.

28. M.I.A. Othman, R.S. Tantawi, *The effect of a laser pulse and gravity field on a thermoelastic medium under Green–Naghdi theory*, Acta Mechanica, **227**, 3571–3583, 2016.

29. A.S. El-Karamany, M.A. Ezzat, *On the phase-lag Green–Naghdi thermoelasticity theories*, Applied Mathematical Modelling, **40**, 5643–5659, 2016.

30. M.N. Allam, K.A. Elsibai, A.E. Abouelregal, *Electromagneto-thermoelastic problem in a thick plate using Green and Naghdi theory*, International Journal of Engineering Science, **47**, 5-6, 680–690, 2009.

31. M.A. Ezzat, A.S. El-Karamany, A.A. Bary, *State space approach to one-dimensional magneto-thermoelasticity under the Green–Naghdi theories*, Canadian Journal of Physics, **87**, 867–878, 2009.

32. Y Jiangong, X. Tonglong, *Generalized thermoelastic waves in spherical curved plates without energy dissipation*, Acta Mechanica, **212**, 39–50, 2010.

33. Y. Jiangong, Z. Xiaoming, X. Tonglong, *Generalized thermoelastic waves in functionally graded plates without energy dissipation*, Composite Structures, **93**, 32–39, 2010.

34. S.Y. Atwa, *Generalized magneto-thermoelasticity with two temperature and initial stress under Green–Naghdi theory*, Applied Mathematical Modelling, **38**, 21-22, 5217–5230, 2014.

35. A.M. Zenkour, *Refined two-temperature multi-phase-lags theory for thermomechanical response of microbeams using the modified couple stress analysis*, Acta Mechanica, **229**, 9, 3671–3692, 2018.

36. A.M. Zenkour, *Refined microtemperatures multi-phase-lags theory for plane wave propagation in thermoelastic medium*, Results in Physics, **11**, 929–937, 2018.

37. A.M. Zenkour, *Refined multi-phase-lags theory for photothermal waves of a gravitated semiconducting half-space*, Composite Structures, **212**, 346–364, 2019.

38. A.M. Zenkour, *Effect of thermal activation and diffusion on a photothermal semiconducting half-space*, Journal of Physics and Chemistry of Solids, **132**, 56–67, 2019.

39. A.M. Zenkour, *Thermal-shock problem for a hollow cylinder via a multi-dual-phase-lag theory*, Journal of Thermal Stresses, **43**, 6, 687–706, 2020.

40. A.M. Zenkour, *Magneto-thermal shock for a fiber-reinforced anisotropic half-space studied with a refined multi-dual-phase-lag model*, Journal of Physics and Chemistry of Solids, **137**, 109213, 2020.

41. D.S. Mashat, A.M. Zenkour, *Modified DPL Green–Naghdi theory for thermoelastic vibration of temperature-dependent nanobeams*, Results in Physics, **16**, 102845, 2020.

42. A.M. Zenkour, *Exact coupled solution for photothermal semiconducting beams using a refined multi-phase-lag theory*, Optics & Laser Technology, **128**, 106233, 2020.

43. M.I.A. Othman, S.Y. Atwa, R.M. Farouk, *The effect of diffusion on two-dimensional problem of generalized thermoelasticity with Green–Naghdi theory*, International Communications Heat Mass Transfer, **36**, 857–864, 2009.

44. B. Singh, *Wave propagation in a Green–Naghdi thermoelastic solid with diffusion*, International Journal of Thermophysics, **34**, 553–566, 2013.

45. S. Deswal, K.K. Kalkal, *Electromagneto-thermodiffusive problem for short times without energy dissipation*, Journal of Engineering Physics and Thermophysics, **86**, 3, 705–715, 2013.

46. S.M. Hosseini, J. Sladek, V. Sladek, *Two dimensional transient analysis of coupled non-Fick diffusion–thermoelasticity based on Green–Naghdi theory using the meshless local Petrov–Galerkin (MLPG) method*, International Journal of Mechanical Sciences, **82**, 74–80, 2014.

47. J.J. Tripathi, G.D. Kedar, K.C. Deshmukh, *Generalized thermoelastic diffusion problem in a thick circular plate with axisymmetric heat supply*, Acta Mechanica, **226**, 2121–2134, 2015.

48. B. Singh, L. Singh, S. Deswal, *Reflection of plane waves in thermo-diffusion elasticity without dissipation under the effect of rotation*, Mechanics of Advanced Materials and Structures, **23**, 1, 74–79, 2016.

49. Q. Xiong, X. Tian, *Transient magneto-thermo-elasto-diffusive responses of rotating porous media without energy dissipation under thermal shock*, Meccanica, **51**, 2435–2447, 2016.

50. M. Aouadi, F. Passarella, V. Tibullo, *A bending theory of thermoelastic diffusion plates based on Green-Naghdi theory*, European Journal of Mechanics – A/Solids, **65**, 123–135, 2017.

51. M. Aouadi, M. Ciarletta, G. Iovane, *A porous thermoelastic diffusion theory of types II and III*, Acta Mechanica, **228**, 931–949, 2017.

52. B. Lazzari, R. Nibbi, *Energy decay in Green–Naghdi thermoelasticity with diffusion and dissipative boundary controls*, Journal of Thermal Stresses, **40**, 7, 917–927, 2017.